DOI: 10.1002/ejic.200900265

Mononuclear and Dinuclear Ni^{II} and Cu^{II} Complexes with a Pyrrolecarboxamide Ligand: Core Conversions and Unusual Presence of a Dimer and Two Monomers in the Same Unit Cell

Jyoti Singh,[a] Geeta Hundal,[b] and Rajeev Gupta*[a]

Keywords: N ligands / Nickel / Copper / H bonding

A potential tetradentate pyrrolecarboxamide ligand, H_4L^1, coordinates to metal ions (M = Ni or Cu) either in tetra-anionic or trianionic fashion to afford mononuclear $[M(L^1)]^{2-}$, dinuclear $[M_2(HL^1)_2]^{2-}$, or adduct $[\{M_2(HL^1)_2\}\{M(L^1)\}_2]^{6-}$ complexes, respectively. The dinuclear complexes can be converted into the mononuclear complexes by the addition of NaOH due to the presence of protonated sites. On the other hand, Cu-monomer can be converted into the Cu adduct after treating with water. Interestingly, the crystal structure of the adduct shows the unusual presence of a Cu_2-dimer and two Cu-monomers in the same unit cell. The structure shows extensive network of H-bonds between the Cu_2-dimer and Cu-monomers through two water molecules. Further, this adduct can be assembled by mixing isolated one mole of Cu_2-dimer and two moles of Cu-monomers. Crystallographic studies depict several interesting weak interactions in these complexes.

Introduction

The importance of new nitrogen-containing ligands in the field of coordination and bioinorganic chemistry has emerged from the presence of such moieties as supporting ligands in several metalloproteins and metalloenzymes.[1] The imidazole ring from the histidine residue is a common ligand found at the active sites of metalloenzymes.[2] Similarly, the identification of deprotonated carboxamide-*N* coordination in certain metalloenzymes has also attracted the synthetic chemists to implement the amide functional groups in the ligand design.[3] In this context, the amide-based ligands containing additional *N*-donors in a multidentate ligand are of particular interests.[4] Our group has been working on the amide-based ligands additionally supported by the neutral amine donors either in macrocyclic ligands[5a] or their open-chain analogues[5b,5c] (Scheme 1). Using these ligands, we have recently shown detailed structural and redox investigations of the Ni^{2+}/Ni^{3+} complexes in a square-planar environment.[5a,5b]

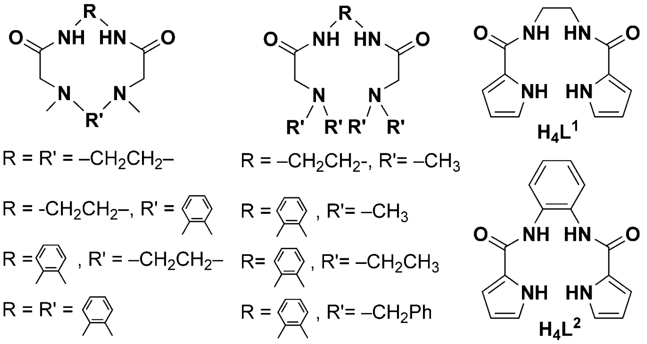

Scheme 1. Ligands discussed and used in this work.

In pursuit of designing new amide-based ligands that will additionally incorporate better donor sites than the neutral amine donors, we were encouraged to introduce pyrrole functionality to develop a new set of ligands that utilize a different approach to the tetraanionic σ-only donation. To this end, η^1-pyrrolyl-based ligands appeared to be promising alternatives. This move was further supported by the recent examples of interesting coordination chemistry with pyrrole-based ligands.[6,7] Furthermore, pyrrole functional group has rarely been used in conjunction with an amide group and we anticipated rich coordination chemistry with such hybrid ligands.[8] Pyrrole-based ligands contain two competing systems involving the nitrogen lone pair: delocalization of the nitrogen lone pair into the aromatic π-system of the pyrrole ring and nitrogen-to-metal π-donation. This competition greatly decreases the amount of donation from the pyrrolyl nitrogen relative to other anionic σ-donor ligands.[6a] However, this route suited our approach as the present set of ligands may not significantly differ from our earlier ligands containing neutral N_{amine} besides N_{amide} donors.[5] The ligands H_4L^1 {bis[2-(1*H*-pyrrol-2-carboxamido)ethylenediamine]} and H_4L^2 {bis[2-(1*H*-pyrrol-2-carboxamido)-*o*-phenylenediamine]} (Scheme 1) were synthesized in a single step by treating the diamine with pyrrole-2-carboxyilic acid and contain either a flexible

---

[a] Department of Chemistry, University of Delhi,
Delhi 110007, India
Fax: +91-11-2766-6605
E-mail: rgupta@chemistry.du.ac.in
[b] Department of Chemistry, Guru Nanak Dev University,
Amritsar, Punjab 143005, India
Supporting information for this article is available on the WWW under http://dx.doi.org/10.1002/ejic.200900265.

ethylene backbone in former or rigid *o-phenylene* backbone in latter. We anticipate that the presence of a flexible backbone in H_4L^1 or rigid backbone in H_4L^2 may result in different coordination mode towards metal ion.

Results and Discussion

The Monomers

The mononuclear Ni^{2+} and Cu^{2+} complexes **1** and **2** were synthesized by treating the ligand H_4L^1 with 4 equiv. of NaH followed by the addition of M^{2+} salt. The absence of ν_{N-H} stretches and the bathochromic shift for the amidate $\nu_{C=O}$ group than the free ligand, confirms the coordination through deprotonated N_{amide}[5,9] The complexes **1** and **2** are isostructural in nature as revealed by their superimposable IR spectra. ^1H NMR spectrum of **1** provided the solution state structure of the Ni^{2+} complex and display sharp peaks with small differences in chemical shifts compared to the free ligand (Figure S1, Supporting Information). The ethylene protons H^4 were observed at about 3.1 ppm whereas pyrrole protons (H^1, H^2, and H^3) between 5.5–6.5 ppm as singlet. The solution state magnetic moment[10a] of the complex **2** was found to be 1.82 μ_B as expected for a magnetically dilute Cu^{II} ion.[10] The absorption spectra of nickel (**1**) and copper (**2**) complexes are shown in Figure 1. Both these complexes show distinct features for the four-coordinate square-planar geometry. For complexes **1** and **2**, the λ_{max} was observed at 417 and 492 nm accompanied by a low-energy shoulder at 471 and 762 nm, respectively. The low ε value for these features suggests the *d–d* transition nature of the peaks. The 1:2 electrolytic nature of complexes **1** and **2** were confirmed by the solution conductivity measurements.[11]

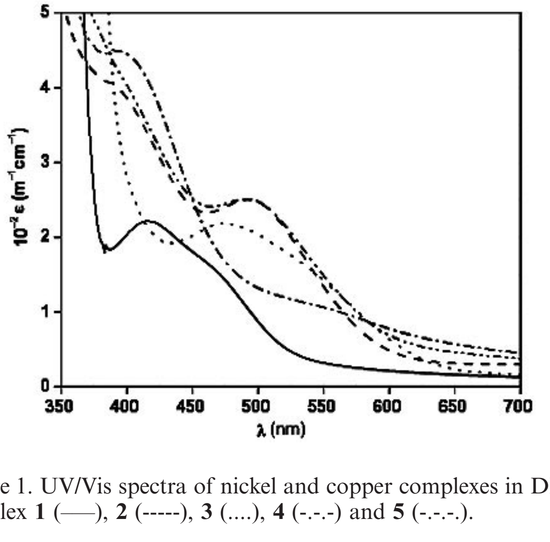

Figure 1. UV/Vis spectra of nickel and copper complexes in DMF: complex **1** (——), **2** (-----), **3** (....), **4** (-.-.-) and **5** (-.-.-.).

The Dimers

The dinuclear Ni_2 and Cu_2 complexes **3** and **4** were synthesized by treatment of ligand H_4L^1 with 3 equiv. of NaH followed by the addition of M^{2+} salt. The presence of ν_{N-H} stretching frequency for **3** (3223 cm^{-1}) and **4** (3214 cm^{-1}) suggests the partial protonated nature of the ligand.[5,9] The complexes **3** and **4** behaved as 1:2 electrolytes as confirmed by the solution conductivity.[11] The ^1H NMR spectrum of **3** also reveals the N–H group at 8.7 ppm which is absent for complex **1** (Figure S1, Supporting Information). The different chemical environments of the two pyrrole rings resulted in the protons (H^1, H^2 and H^3) for the pyrrole ring connected to the deprotonated amide group being more upfield shifted than the ones (H^5, H^6 and H^7) that are next to the protonated amide group. The observed similarities of the protons H^1, H^2 and H^3 in **3** with that of monomer **1** suggest a similar chemical environment of two moieties (cf. crystal structures). As observed for the mononuclear complexes **1** and **2**, the complexes **3** and **4** are also isostructural in nature as observed by their super-imposable IR spectra. The solution state magnetic moment[10a] of the complex **4** was found to be $1.23\mu_{B/Cu}$ and indicate a moderately strong antiferromagnetic coupling between two Cu^{II} ions.[10b,12] Although the intramolecular Cu···Cu distance (6.779–6.970 Å) in the dimer complex is on the higher side, a moderate antiferromagnetic coupling can not be ruled out. The solid state EPR spectrum (Figure S7) of complex **4** displays a broad undefined signal at $g = 2.132$ with ΔH_{p-p} of 136 G. However, the solution state spectrum (Figure 2) clearly shows 7 lines features due to the dimeric nature of the copper complex.[8b,13] The absorption spectra of Ni_2 (**3**) and Cu_2 (**4**) dimers (Figure 1) display λ_{max} at 477 and 550 nm accompanied with several low-energy shoulders. The low ε value for these features suggests the *d–d* transition nature of the peaks.

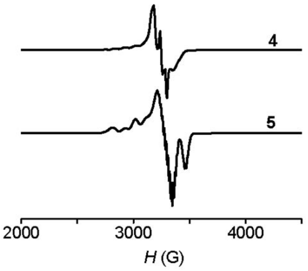

Figure 2. Solution state EPR spectra of complexes **4** and **5** at 120 K.

The molecular structure of complex **4** is shown in Figure 3 whereas the important crystallographic and bond angles and bond lengths are contained in Table 3 and Table 1, respectively. The unit cell contains two crystallographically independent dimeric molecules. Each Cu^{2+} ion is coordinated by two deprotonated $N_{pyrrole}$ (avg. 1.928 Å), one deprotonated N_{amide} (avg. 1.935 Å) and one O_{amide} (avg. 2.017 Å) in a N_3O plane which deviates significantly from planarity, maximum deviation being 0.25 and 0.22 Å for molecule 1 and molecule 2 (containing Cu1 and Cu2), respectively. The Cu1 and Cu2 ions are lying 0.01 and 0.03 Å above these planes. These two molecules are lying perpendicular to each other (dihedral angle between two

Cu planes is 88°) and held together by N–H···O and various C–H···O and C–H···N type H-bonding interactions (Table S1). These interactions between two molecules form linear undulating anionic chains running diagonally in the *bc* plane (Figure S2, Supporting Information) which is supplemented by the C–H···π interactions between pyrrole ring containing N1 of molecule 1 and C15 atom belonging to the molecule 2 (C15–H15···centroid distance: 4.08 Å). These undulating anionic chains are alternately packed with similar undulating cationic chains of Et_4N^+ cations (Figure 4, S3, and S4). Thus, the Et_4N^+ cations are efficiently occupying the space created in between the parallel anionic chains and are being held in place by various C–H···O and C–H···N-type weak H-bonds between the alkyl groups of Et_4N^+ and O and N atoms of the ligand.

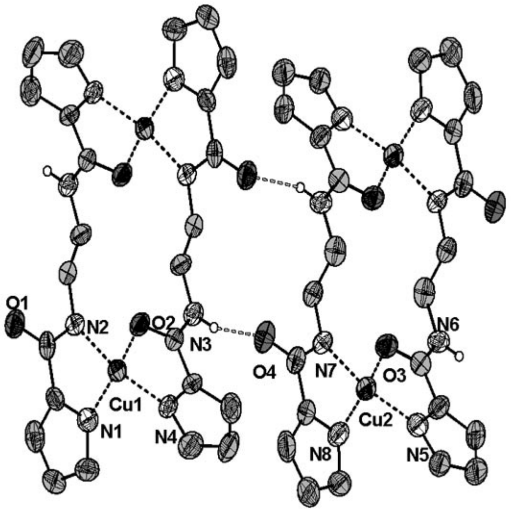

Figure 3. Thermal ellipsoidal representation (50% probability level with partial numbering scheme) of complex **4**. Hydrogen atoms, except amide protons, and cations have been omitted for clarity.

Table 1. Selected bond lengths [Å] and angles [°] for $(Et_4N)_2[Cu_2(HL^1)_2]\cdot H_2O$ (**4**).

Bond lengths/bond angles Molecule **1**		Molecule **2**	
Cu1–N1	1.918(5)	Cu2–N5	1.941(6)
Cu1–N2	1.947(5)	Cu2–N7	1.923(6)
Cu1–N4	1.932(5)	Cu2–N8	1.920(6)
Cu1–O2	2.008(4)	Cu2–O3	2.026(5)
C5–O1	1.277(7)	C17–O3	1.278(8)
C8–O2	1.270(7)	C20–O4	1.259(8)
N2–C5	1.339(8)	N6–C17	1.334(9)
N3–C8	1.325(8)	N7–C20	1.332(9)
N1–Cu1–N4	100.9(2)	N5–Cu2–N8	100.7(2)
N1–Cu1–N2	84.0(2)	N7–Cu2–N8	84.2(2)
N2–Cu1–O2	96.55(19)	N5–Cu2–O3	82.7(2)
N4–Cu1–O2	81.65(19)	N7–Cu2–O3	94.7(2)
N1–Cu1–O2	166.8(2)	N8–Cu2–O3	167.5(2)
N2–Cu1–N4	166.1(2)	N5–Cu2–N7	168.4(2)

Interestingly, a similar looking structure for a dinuclear copper(I) complex with a proline-amide based tetradentate ligand has been reported by Iglesias et al.[14] The Cu^I–N_{amine}, Cu^I–N_{amide}, and Cu^I–O_{amide} distances are reported to be in the range of 1.91–1.98 Å, 1.79–1.94 Å, and 1.90–2.02 Å, respectively. It may be noted, however, that the neutral tetradentate ligand was used in the synthesis of the dinuclear Cu^I_2 complex, in complete contrast to that of **4** where a partially deprotonated ligand has been used.

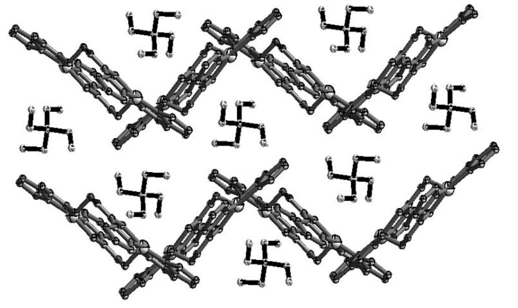

Figure 4. Packing of anionic chains of complex **4** and Et_4N^+ cations.

The Monomer–Dimer Adduct

Complex **5**, essentially a 2:1 mixture of complexes **2** and **4**, was formed by treating ligand H_4L^1 with 3.5 equiv. of NaH followed by the addition of Cu^{2+} salt and a few drops of water. Our observation suggests that the presence of small amount of water during the synthesis is crucial for the isolation of this compound. This observation is well corroborated by the crystal structure analysis (vide infra) that shows the presence of water molecules in the lattice, FTIR spectra, and microanalysis results. The IR spectrum of complex **5** is essentially composed of combined features for complexes **2** and **4**. For example, the unique $\nu_{C=O}$ stretches for complexes **2** and **4** at 1540 and 1590 cm^{-1}, respectively, are observable simultaneously in the IR spectrum.[5,9] The solution state magnetic moment[10a] of the complex **5** ($1.53\mu_{B/Cu}$) was found to be lower than **2** but higher than **4** and indicate a moderate antiferromagnetic coupling between two Cu^{II} ions.[10b,12,15] This is not completely unexpected as the adduct complex **5** is composed of two un-coupled monomeric and one coupled dimeric sites simultaneously. The 1:6 electrolytic nature of **5** was confirmed by the solution conductivity.[11] The adduct complex **5** show combined absorption spectral features of Cu-monomer and Cu_2-dimer and composed of λ_{max} at 406 and 492 nm with a shoulder at 762 nm (Figure 1). The solid state EPR spectra of complex **5** displays a broad undefined signal at $g = 2.088$ (with $\Delta H_{p\text{-}p} = 82$ G) as also observed for the complex **4** (Figure S7). Interestingly, the solution spectrum is quite complex presumably due to the presence of both dimeric as well as monomeric units (Figure 2).[13]

The complex **5** was crystallographically characterized and reveals a number of interesting features. The crystal structure of complex **5** is shown in Figure 5 whereas the important crystallographic details and bond angles and bond lengths are contained in Tables 3 and 2, respectively. Importantly, the lattice shows the presence of one dinuclear (**4–Cu₂**) and two mononuclear (**2–Cu**) fragments in the unit cell.[16] The **4–Cu$_2$** and **2–Cu** fragments are involved in extensive hydrogen-bonding network through two water molecules. The Cu^{2+} ion in **2–Cu** is surrounded by two deprotonated $N_{pyrrole}$ (avg. 1.952 Å) and two deprotonated N_{amide} (avg. 1.924 Å) in a distorted square-planar fashion. The average Cu–$N_{pyrrole}$ bond is ca. 0.03 Å longer than the average Cu–N_{amide} bond. The N_{amide}–Cu–N_{amide} bond angle is about 28° smaller than the $N_{pyrrole}$–Cu–$N_{pyrrole}$ angle. For **2–Cu**, the displacement of the copper ion from the N_4 basal plane is 0.131 Å. As observed for the structure of **4**, the copper ion of the dinuclear fragment **4–Cu$_2$** is coordinated by two deprotonated $N_{pyrrole}$ (avg. 1.924 Å), one deprotonated N_{amide} (1.936 Å), and one O_{amide} (1.978 Å). For **4–Cu$_2$** the Cu–O_{amide} bond length is 0.04 Å shorter than in **4**. The geometry around the Cu^{II} ion is distorted square-planar with the displacement from the N_3O basal plane being 0.093 Å.

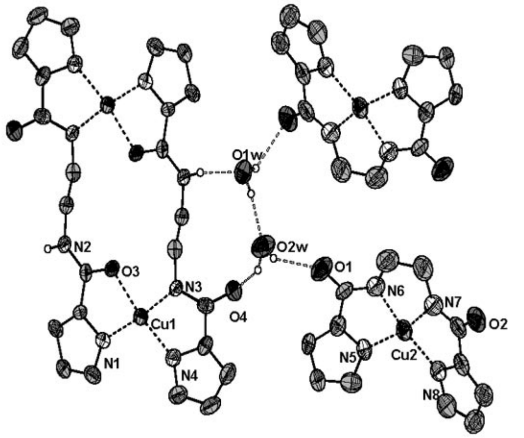

Figure 5. Thermal ellipsoidal representation (50% probability level with partial numbering scheme) of complex **5**. Hydrogen atoms, except amide protons, and cations have been omitted for clarity.

Table 2. Selected bond lengths [Å] and angles [°] for $(Et_4N)_6[Cu(L^1)]_2[Cu_2(HL^1)_2]\cdot 6H_2O$ (**5**).

Bond lengths/bond angles Dimer (**4-Cu$_2$**)		Monomer (**2-Cu**)	
Cu1–N1	1.940(6)	Cu2–N5	1.967(6)
Cu1–N3	1.936(5)	Cu2–N6	1.919(8)
Cu1–N4	1.908(7)	Cu2–N7	1.929(6)
Cu1–O3	1.978(5)	Cu2–N8	1.937(7)
C5–O3	1.271(9)	C17–O1	1.241(10)
C10–O4	1.289(9)	C20–O2	1.279(10)
N1–Cu1–O3	82.6(2)	N5–Cu2–N6	83.1(3)
N3–Cu1–O3	91.7(2)	N6–Cu2–N7	82.5(3)
N3–Cu1–N4	84.4(3)	N7–Cu2–N8	83.2(3)
N1–Cu1–N4	101.2(3)	N5–Cu2–N8	110.1(3)
N1–Cu1–N3	174.3(3)	N5–Cu2–N7	163.0(3)
N4–Cu1–O3	169.4(2)	N6–Cu2–N8	164.9(3)

Two water molecules are H-bonded with each other and further connect the dimer with two monomers to generate a linear chain running diagonally across the *ab* plane (Figure S5). Strong H-bonding interactions exist between the water dimer, O_{amide} atoms O1, O2 and O4 and N_{amide} N2. These anionic parallel chains, running across the *ab* plane are interspersed with Et_4N^+ cations being sandwiched. Thus, these cations are held in place due to many weak C–H···O type H-bonds between the anionic and the cationic layers (Figure 6 and S6, Table S2). There are also present various C–H···π interactions between the pyrrole rings and Et_4N^+ cations with centroid to C distances of 3.494–3.778 Å.

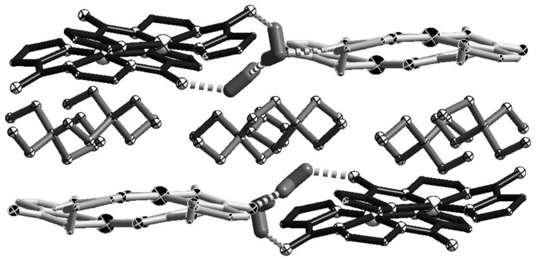

Figure 6. Packing of anionic chains of complex **5** and Et_4N^+ cations.

Core Conversion Studies

The inherent flexible nature of the ligand H_4L^1 prompted us to attempt conversion of the dimers to the monomers and vice versa (Scheme 2). Interestingly, dimers **3** and **4** can be converted to monomers **1** and **2**, respectively, by deprotonating the remaining amide N–H groups. NaOH was used for this purpose: whereas 2 equiv. was sufficient for the

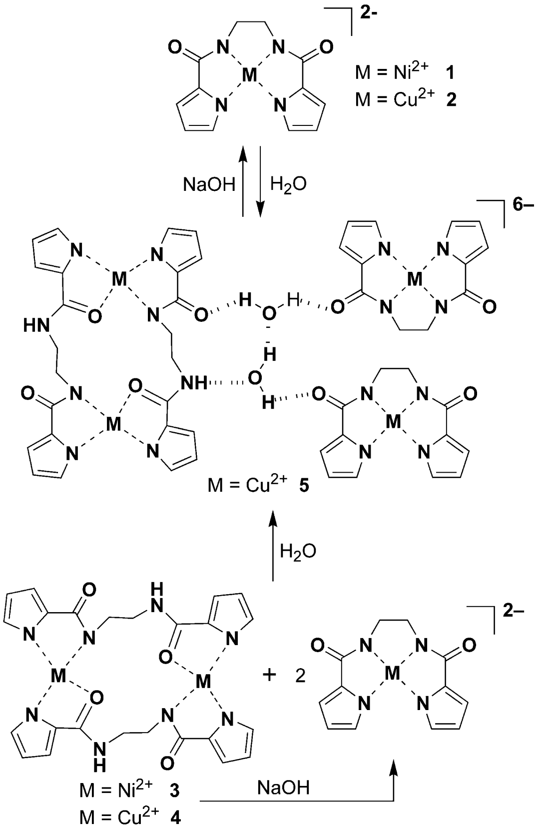

Scheme 2. Metal complexes and their interconversion.

conversion of **4** to **2**; 12 equiv. were required for the analogous nickel complex **3**. The adduct **5** can also be assembled by mixing two molecules of **2** and one molecule of **4** in DMF in presence of small amount of water. As discussed before, presence of water is crucial for the adduct formation due to engagement in H-bond formation that connects monomers to the dimer. Furthermore, the adduct **5** can also be synthesized directly by treating Cu-monomer **2** with 10 equiv. of H_2O as it most likely results in the partial protonation of the ligand. This may be noted that the similar reaction involving Ni-monomer **1** resulted in decomposition and clearly suggest the difference associated with the acid/base strength of the amide groups in copper and nickel complexes.

Conclusions

The inherent flexibility of the ethylene bridge in H_4L^1 has resulted in various coordination modes of the ligand to afford mononuclear, dinuclear, and adduct complexes. Interestingly, the monomer, dimer and adduct core formation can be controlled by the selection/addition of a suitable acid or base. In contrast, the ligand H_4L^2 only affords mononuclear Cu^{II} and Ni^{II} complexes.[17] Further studies are in progress to understand the proton-regulated electron transfer reactions in these complexes as the monomer, dimer and adduct cores differ only in the number of protonic sites available in the complexes.

Experimental Section

Materials and Reagents: All reagents were obtained from the commercial sources and used as received. *N*,*N*-dimethylformamide (DMF) was dried and distilled from molecular sieves (4 Å) and was stored over sieves. Pyridine was distilled from KOH pellets. Methyl alcohol (CH_3OH) was distilled from magnesium methoxide. Acetonitrile (MeCN) was dried by distillation from anhydrous CaH_2. Diethyl ether was dried by refluxing over sodium metal under inert atmosphere followed by distillation. Dichloromethane (CH_2Cl_2) was purified by washing with 5% sodium carbonate solution followed by water and finally dried with anhydrous $CaCl_2$, before a final reflux and distillation. *o*-phenylenediamine was recrystallized from dichloromethane.

Physical Measurements: The conductivity measurements were done in organic solvents using the digital conductivity bridge from the Popular Traders, India (model number: PT-825). The elemental analysis data were obtained from the Elementar Analysen Systeme GmbH Vario EL-III instrument. The NMR spectral measurements were done using an Avance Bruker (300 MHz) instrument. The infra-red spectra (either as KBr pellet or as a mull in mineral oil) were recorded using the Perkin–Elmer FTIR–2000 spectrometer. The absorption spectra were recorded using the Perkin–Elmer Lambda-25 spectrophotometer. Solution magnetic susceptibility measurements were made by the Evan's NMR method.[10a] Diamagnetic correction were made according to the standard text.[10b] EPR spectra of the polycrystalline samples or solutions were recorded at X-band (9.455 GHz) frequencies with a Bruker EMX 1444 EPR spectrometer at 120 K. The EPR spectra were calibrated with diphenylpicrylhydrazyl (DPPH) radical ($g = 2.0037$).

Crystallography: Single crystals suitable for X-ray diffraction studies were grown by the vapour diffusion of diethyl ether to a DMF solution of complex **4** and **5**. The suitable crystals of **4** and **5** were mounted lengthways with the largest dimension in a sealed capillary. The intensity data for complexes **4** and **5** were collected at 295 K on a Bruker Kappa Apex CCD detector with graphite monochromatized Mo-K_α radiation.[18] For complex **4**, a total of 27552 reflections were measured of which 6698 were unique and 3658 were considered observed [$I > 2\sigma(I)$]. For complex **5**, total of 14937 reflections were measured of which 5956 were unique and 3603 were considered observed [$I > 2\sigma(I)$]. The data were corrected for Lorentz and polarization effects and a psi-scan absorption correction was also applied. The structures were solved by the direct methods using SIR-92[19] and refined by full-matrix least-squares refinement techniques on F^2 using SHELXL97.[20] All calculations were done using Wingx software.[21] All non-hydrogen atoms were refined anisotropically. Hydrogen atoms of the water molecule were located from the difference Fourier map and were not refined. All other hydrogen atoms were fixed geometrically with U_{iso} values of 1.2 times (for methylene and aromatic carbons) and 1.5 times (methyl carbons) the U_{iso} values of their respective carrier atoms. Details of the crystallographic data are given in Table 3. CCDC-724513 (for complex **4**) and -724512 (for complex **5**) contain the crystallographic data for this paper. These data can be obtained free of charge from The Cambridge Data Center via www.ccdc.cam.ac.uk/data_request/cif.

Table 3. Crystallographic data for $(Et_4N)_2[Cu_2(HL^1)_2]\cdot H_2O$ (**4**) and $(Et_4N)_6[Cu(L^1)]_2[Cu_2(HL^1)_2]\cdot 6H_2O$ (**5**).

	4	**5**
Empirical formula	$C_{40}H_{62}Cu_2N_{10}O_4$	$C_{96}H_{170}Cu_4N_{22}O_{12}$
Formula mass	874.08	2078.74
Crystal system	triclinic	triclinic
Space group	$P\bar{1}$	$P\bar{1}$
Color, shape	brown, block	brown, block
Size /mm	$0.18 \times 0.16 \times 0.16$	$0.18 \times 0.16 \times 0.12$
a /Å	9.5960(2)	13.612(7)
b /Å	15.3190(3)	13.745(7)
c /Å	16.0480(2)	15.675(8)
α /°	112.080(1)	103.87(3)
β /°	91.430(2)	92.54(3)
γ /°	91.917(2)	108.58(3)
V /Å^3	2183.04(7)	2676(2)
Z	2	1
$F(000)$	924	1112
$D_{calcd.}$ /g cm^{-3}	1.330	1.290
Absorption coefficient /mm^{-1}	1.025	0.850
R[a]	0.0697	0.0625
R_w[b]	0.2005	0.1576
GOF on F^2	0.978	1.038

[a] $R = \Sigma||F_o| - |F_c||/\Sigma|F_o|$. [b] $R_w = \{[\Sigma(|F_o|^2|Fc|^2)^2]\}^{1/2}$.

Synthesis of Ligands

Synthesis of H_4L^1: To a solution of pyrrole-2-carboxylic acid (2.0 g, 18 mmol) in 7 mL of pyridine was added ethylenediamine (0.54 g, 9 mmol) and triphenylphosphite (5.58 g, 18 mmol) with stirring. The resulting mixture was heated with stirring at 80 °C overnight. Excess pyridine was removed under reduced pressure followed by the addition of 20 mL of dichloromethane. This resulted in the precipitation of a white solid. The resultant mixture was filtered and washed with water followed by diethyl ether. The crude compound was recrystallized from methanol; yield 1.4 g (63%). $C_{12}H_{14}N_4O_2$ (246.27): calcd. C 58.53, H 5.73, N 22.75; found C 57.99, H 6.25, N 22.64. ^{1}H NMR spectrum (300 MHz, [D$_6$]DMSO, 25 °C): δ = 3.6 (d, 4 H, -CH$_2$-CH$_2$-), 6.2 (s, 2 H, pyrrole), 6.9 (s, 4 H, pyrrole), 8.1 (s, 2 H, br, NH), 11.6 (s, 2 H, NH-py) ppm. FTIR spectrum (KBr): $\tilde{\nu}$ = 3400 (s), 3300 (s), 3118 (m), 2983 (m), 2943 (m), 1623 (s) cm^{-1}.

Synthesis of H_4L^2: This ligand was synthesized in a similar manner as for H_4L^1 with following reagents: pyrrole-2-carboxylic acid (2.0 g, 18 mmol), *o*-phenylenediamine (0.97 g, 9 mmol) and triphenylphosphite (5.58 g, 18 mmol); yield 1.4 g (53%). $C_{16}H_{14}N_4O_2$ (294.31): calcd. C 65.30, H 4.79, N 19.04; found C 64.78, H 5.50, N 19.73. ^{1}H NMR spectrum (300 MHz, [D$_6$]DMSO, 25 °C): δ = 6.18 (s, 2 H, pyrrole), 6.93 (s, 4 H, pyrrole), 7.18 (s, 2 H, Ar-H), 7.65 (s, 2 H, Ar-H), 9.74 (s, 2 H, br, NH), 11.30 (br. s, 2 H, NH-Py) ppm. FTIR spectrum (KBr): $\tilde{\nu}$ = 3412 (s), 3297 (s), 3259 (m), 1669 (s), 1614 (s) cm^{-1}.

General Synthetic Procedure for the Mononuclear Complexes: The ligand H_4L^1 (0.05 g, 0.20 mmol) was dissolved in 3 mL of DMF and treated with solid NaH (0.019 g, 0.80 mmol) under dinitrogen atmosphere. The mixture was stirred until H_2 evolution was ceased (ca. 5–10 min). To this mixture was added a 0.20 mmol solution of $(Et_4N)_2[MCl_4]$ (M^{II} = Cu or Ni) in 5 mL of DMF under inert atmosphere. The resulting mixture was further stirred for 1 h at room temperature.

$(Et_4N)_2[NiL^1]\cdot H_2O$ (1): After 1 h stirring, the solvent was removed under reduced pressure. The resultant yellow solid was dissolved in CH_3CN and passed through a pad of celite in a medium porosity frit. The filtrate was then subjected to the diethyl ether diffusion to afford the yellow crystalline product; yield 0.08 g (72%). $C_{28}H_{52}N_6O_3Ni\cdot H_2O$ (579.9): calcd. C 57.94, H 8.96, N 14.48; found C 58.06, H 9.26, N 14.48. FTIR spectrum (KBr): $\tilde{\nu}$ = 3369 (m), 2980 (m), 2926 (m), 2850 (m), 1545 (s) cm^{-1}. Conductivity (DMF, ca. 1 mM solution, 298 K): Λ_M = 150 Ω^{-1} cm^2 mol^{-1} (1:2 electrolyte). UV/Vis spectrum [λ_{max}, nm (ε, M^{-1} cm^{-1})] (in DMF): 471 (sh, 120), 417 (220), 336 (9000), 320 (8400). ^{1}H NMR spectrum (400 MHz, [D$_6$]DMSO, 25 °C): δ = 1.15 (t, J = 7.16 Hz, 24 H, Et$_4$N-CH$_3$), 3.08 (s, 4 H, H^4), 3.26 (s, 16 H, Et$_4$N-CH$_2$), 5.69 (s, 2 H, H^2), 6.08 (s, 2 H, H^3), 6.38 (s, 2 H, H^1) ppm.

$(Et_4N)_2[CuL^1]\cdot 3H_2O$ (2): This resultant light red solution was filtered through a pad of celite in a medium porosity frit. The filtrate was directly subjected to the diethyl ether diffusion to afford light red blocks; yield 0.08 g (70%). $C_{28}H_{56}N_6O_5Cu\cdot 3H_2O$ (620.75): calcd. C 54.10, H 9.02, N 13.53; found C 54.42, H 9.06, N 13.27. FTIR spectrum (KBr): $\tilde{\nu}$ = 3403 (m), 2976 (m), 2939 (m), 1544 (s) cm^{-1}. Conductivity (DMF, ca. 1 mM solution, 298 K): Λ_M = 160 Ω^{-1} cm^2 mol^{-1} (1:2 electrolyte). UV/Vis spectrum [λ_{max}, nm (ε, M^{-1} cm^{-1})] (in DMF): 762 (sh, 30), 492 (250), 406 (sh, 360), 293 (20500). μ_{eff} (DMF, 298 K) = 1.82 B.M..

General Synthetic Procedure for Dinuclear Complexes: The ligand H_4L^1 (0.05 g, 0.20 mmol) was dissolved in 3 mL of DMF and treated with solid NaH (0.015 g, 0.60 mmol) under dinitrogen atmosphere. The mixture was stirred until H_2 evolution was ceased (ca. 5–10 min). To this mixture was added a 0.20 mmol solution of $(Et_4N)_2[MCl_4]$ (M^{II} = Cu or Ni) in 5 mL of DMF under inert atmosphere. The resulting mixture was further stirred for 2 h at room temperature.

$(Et_4N)_2[Ni_2(HL^1)_2]\cdot H_2O$ (3): The resultant red-orange solution was filtered through a pad of celite in a medium porosity frit and the filtrate was directly subjected to the vapour diffusion of diethyl ether. This afforded a dark red crystalline product within one day; yield 0.04 g (45%). $C_{40}H_{64}N_{10}O_5Ni_2\cdot H_2O$ (881.38): calcd. C 54.46, H 7.26, N 15.88; found C 54.67, H 7.26, N 15.88. FTIR spectrum (KBr): $\tilde{\nu}$ = 3223 (m), 3068, 3000 (w), 2935 (m), 1608 (s), 1542 (s) cm^{-1}. Conductivity (DMF, ca. 1 mM solution, 298 K): Λ_M = 150 Ω^{-1} cm^2 mol^{-1} (1:2 electrolyte). UV/Vis spectrum [λ_{max}, nm (ε, M^{-1} cm^{-1})] (in DMF): 703 (sh, 20), 557 (sh, 130), 477 (220), 291 (83000). ^{1}H NMR spectrum (300 MHz, [D$_6$]DMSO, 25 °C): δ = 1.15 (t, J = 7.16 Hz, 24 H, Et$_4$N-CH$_3$), 2.99 (s, 8 H, -CH$_2$-H^4), 3.20 (q, J = 7.25 Hz, 16 H, Et$_4$N–CH$_2$), 5.59 (s, 2 H, H^2), 5.87 (s, 4 H, H^3 & H^6), 6.18 (s, 2 H, H^1), 6.51 (s, 2 H, H^5), 6.62 (s, 2 H, H^7), 8.70 (s, 2 H, -NH-C=O) ppm. ^{13}C NMR spectrum (400 MHz, [D$_6$]-DMSO, 25 °C): δ = 7.51 (Et$_4$N-CH$_3$), 51.85 (Et$_4$N-CH$_2$, C^6), 106.29, 106.94 (C^2, C^3), 110.10 (C^{10}), 125.90 (C^1), 131.42 (C^9, C^{10}), 133.27 (C^4, C^8), 140.00 (C^7), 169.34, 171.55 (C=O) ppm.

$(Et_4N)_2[Cu_2(HL^1)_2]\cdot H_2O$ (4): The resultant dark brown solution was filtered through a pad of celite in a medium porosity frit and the filtrate was directly subjected to the diethyl ether diffusion to afford dark brown crystalline product; yield 0.05 g (56%). $C_{40}H_{64}N_{10}O_5Cu_2\cdot H_2O$ (891.08): calcd. C 53.86, H 7.18, N 15.71; found C 54.05, H 7.26, N 15.75. FTIR spectrum (KBr): $\tilde{\nu}$ = 3214 (m), 3105 (w), 2983 (m), 2939 (m), 1597 (s), 1539 (s) cm^{-1}. Conductivity (DMF, ca. 1 mM solution, 298 K): Λ_M = 165 Ω^{-1} cm^2 mol^{-1} (1:2 electrolyte). UV/Vis spectrum [λ_{max}, nm (ε, M^{-1} cm^{-1})] (in DMF): 550 (sh, 110), 406 (440), 296 (23600). EPR spectrum (solid, 120 K): g = 2.178 and 2.086; $\Delta H_{p\text{-}p}$ = 136 G. EPR spectrum (DMF, 120K): g = 2.452, 2.384, 2.295, 2.286, 2.136, 2.075, and 2.050. μ_{eff} (DMF, 298 K) = 1.23 B.M.

Synthesis of Dimer–Monomer Adduct

$(Et_4N)_6[Cu(L^1)]_2[Cu_2(HL^1)_2]\cdot 6H_2O$ (5): To a stirred solution of H_4L^1 (0.05 g, 0.20 mmol) in DMF (10 cm^3), solid NaH (0.017 g, 0.70 mmol) was added under dinitrogen atmosphere. The resulting solution was stirred until H_2 evolution was ceased. To this mixture, a solution of $(Et_4N)_2[CuCl_4]$ (0.94 g, 0.20 mmol) in 5 mL of DMF was added followed by the addition of 10 equiv. of water. The resulting red-brown solution was stirred at room temperature for 2 h. The solution was then passed through a pad of celite in a medium porosity frit. The filtrate was subjected to the vapour diffusion of diethyl ether to afford red-brown colored crystalline product; yield 0.05 g (50%). $C_{96}H_{174}N_{22}O_{16}Cu\cdot 6H_2O$ (2115.37): calcd. C 54.58, H 8.22, N 14.56; found C 53.94, H 8.36, N 14.07. FTIR spectrum (KBr): $\tilde{\nu}$ = 3398 (m), 2978 (m), 2937 (m), 1591 (s), 1538 (s) cm^{-1}. Conductivity (DMF, ca. 1 mM solution, 298 K): Λ_M = 230 Ω^{-1} cm^2 mol^{-1} (calculated for half molecule, 1:3 electrolyte). UV/Vis spectrum [λ_{max}, nm ($\varepsilon_{/Cu}$, M^{-1} cm^{-1})] (in DMF): 762 (sh, 30), 492 (250), 406 (sh, 380), 292 (25100). EPR spectrum (solid, 120 K): g = 2.088; $\Delta H_{p\text{-}p}$ = 82 G. EPR spectrum (DMF, 120 K): g = 2.398, 2.314, 2.236, 2.169, 2.100, 2.031, 2.026, 2.008 and 1.949. μ_{eff} (DMF, 298 K) = 1.53 B.M.

Supporting Information (see also the footnote on the first page of this article): NMR spectra (Figure S1), crystal structures (Figures S2–S6), and EPR spectrum (Figure S7); tables listing H-bonding interactions (Tables S1 and S2).

Acknowledgments

R. G. acknowledges the generous financial support from the University Grant Commission (UGC), University of Delhi under the scheme to strengthen R&D, and the crystallographic help received from IIT-Roorkee (Professor U. P. Singh). J. S. thanks UGC for a fellowship (SRF).

---

[1] a) R. R.Crichton, in: *Biological Inorganic Chemistry*, Elsevier Ltd., Oxford, U. K., **2008**; b) S. J. Lippard, J. M. Berg, in: *Prin-*

ciples of Bioinorganic Chemistry, Panima Corporation, Delhi, India, **2005**; c) R. M. Roat-Malone, in: *Bioinorganic Chemistry*, 2nd ed., John Wiley & Sons, Hoboken, New Jersey, **2007**.

[2] a) T. Tsukihara, H. Aoyama, E. Yamashita, T. Tomizaki, H. Yamaguchi, K. Shinzawa-Itoh, R. Nakashima, R. Yaono, S. Yoshikawa, *Science* **1995**, *269*, 1069; b) S. Iwata, C. Ostermeier, B. Ludwig, H. Michel, *Nature* **1995**, *376*, 660; c) S. T. Prigge, B. A. Eipper, R. E. Mains, L. M. Amzel, *Science* **2004**, *304*, 864; d) K. Harford, B. Sarkar, *Acc. Chem. Res.* **1997**, *30*, 123.

[3] a) C. L. Drennan, T. I. Doukov, S. W. Ragsdale, *J. Biol. Inorg. Chem.* **2004**, *9*, 511; b) W. Huang, J. Jia, J. Cummings, M. Nelson, G. Schneider, Y. Lindqvist, *Structure* **1997**, *5*, 691; c) S. B. Choudhury, J.-W. Lee, G. Davidson, Y.-I. Yim, K. Bose, M. L. Sharma, S.-O. Kang, D. E. Cabelli, M. J. Maroney, *Biochemistry* **1999**, *38*, 3744; d) J. W. Peters, M. H. Stowell, M. Soltis, M. G. Finnegan, M. K. Johnson, D. C. Rees, *Biochemistry* **1997**, *36*, 1181.

[4] a) T. C. Harrop, P. K. Mascharak, *Coord. Chem. Rev.* **2005**, *249*, 3007; b) D.-L. Popescu, A. Chanda, M. Stadler, F. Tiago de Oliveira, A. D. Ryabov, E. Munck, E. L. Bominaar, T. J. Collins, *Coord. Chem. Rev.* **2008**, *252*, 2050; c) R. Ruiz, J. Faus, F. Lloret, M. Julve, Y. Journaux, *Coord. Chem. Rev.* **1999**, *193*, 1069; d) A. K. Patra, R. Mukherjee, *Inorg. Chem.* **1999**, *38*, 1388; e) A. K. Singh, R. Mukherjee, *Dalton Trans.* **2005**, 2886.

[5] a) S. K. Sharma, S. Upreti, R. Gupta, *Eur. J. Inorg. Chem.* **2007**, 3247; b) J. Singh, G. Hundal, R. Gupta, *Eur. J. Inorg. Chem.* **2008**, 2052; c) J. Singh, G. Hundal, M. Corbella, R. Gupta, *Polyhedron* **2007**, *26*, 3893.

[6] a) S. A. Harris, J. T. Ciszewski, A. L. Odom, *Inorg. Chem.* **2001**, *40*, 1987; b) Y. Li, A. Turnas, J. T. Ciszewski, A. L. Odom, *Inorg. Chem.* **2002**, *41*, 6298; c) Y. Shi, C. Cao, A. L. Odom, *Inorg. Chem.* **2004**, *43*, 275; d) Y. Zhang, A. Thompson, S. J. Rettig, D. Dolphin, *J. Am. Chem. Soc.* **1998**, *120*, 13537; e) A. Thompson, S. J. Rettig, D. Dolphin, *Chem. Commun.* **1999**, 631; f) W. H. Harman, C. J. Chang, *J. Am. Chem. Soc.* **2007**, *129*, 15128; g) K. M. Wampler, R. R. Schrock, *Inorg. Chem.* **2007**, *46*, 8463.

[7] a) J. Bachmann, D. G. Nocera, *J. Am. Chem. Soc.* **2005**, *127*, 4730; b) T. E. Wood, N. D. Dalgleih, E. D. Power, A. Thompson, X. Chen, Y. Okamoto, *J. Am. Chem. Soc.* **2005**, *127*, 5740; c) J. L. Sessler, E. Tomat, V. M. Lynch, *J. Am. Chem. Soc.* **2006**, *128*, 4184; d) G. Givaja, M. Volpe, M. A. Edwards, A. J. Blake, C. Wilson, M. Schrider, J. B. Love, *Angew. Chem. Int. Ed.* **2007**, *46*, 584; e) S. A. Carabineiro, L. C. Silva, P. T. Gomes, L. C. J. Pereira, L. F. Veiros, S. I. Pascu, M. T. Duarte, S. Namorado, R. T. Henriques, *Inorg. Chem.* **2007**, *46*, 6880; f) Y. Wang, H. Fu, F. Shen, X. Sheng, A. Peng, Z. Gu, H. Ma, J. S. Ma, J. Yao, *Inorg. Chem.* **2007**, *46*, 3548.

[8] For anion binding, see: a) Z. Yin, Z. Li, A. Yu, J. He, J.-P. Cheng, *Tetrahedron Lett.* **2004**, *45*, 6803. For cation binding see: b) V. S. Thoi, J. R. Stork, E. T. Niles, E. C. Depperman, D. L. Tierney, S. M. Cohen, *Inorg. Chem.* **2008**, *47*, 10533; c) C. L. Weeks, P. Turner, R. R. Fenton, P. A. Lay, *J. Chem. Soc., Dalton Trans.* **2002**, 931.

[9] K. Nakamoto, in: *Infrared and Raman Spectra of Inorganic and Coordination Compounds*, John Wiley & Sons, **1986**.

[10] a) D. F. Evans, *J. Chem. Soc.* **1959**, 2003; b) C. J. O'Connor, *Prog. Inorg. Chem.* **1982**, *19*, 203.

[11] W. J. Geary, *Coord. Chem. Rev.* **1971**, *7*, 81.

[12] a) M. Julve, L. M. Verdaguer, A. Gleizes, M. Philoche-Levisalles, O. Kahn, *Inorg. Chem.* **1984**, *23*, 3808; b) O. Kahn, *Angew. Chem. Int. Ed. Engl.* **1985**, *24*, 834; c) J. L. Shaw, G. T. Yee, G. Wang, D. E. Benson, C. Gokdemir, C. J. Ziegler, *Inorg. Chem.* **2005**, *44*, 5060.

[13] M. K. Saha, D. K. Dey, B. Samanta, A. J. Edwards, W. Clegg, S. Mitra, *Dalton Trans.* **2003**, 488.

[14] M. J. Alcon, E. Gutierrez-Puebla, M. Iglesias, M. A. Monge, F. Sanchez, *Inorg. Chim. Acta* **2000**, *306*, 117.

[15] M. Julve, J. Faus, *J. Am. Chem. Soc.* **1984**, *106*, 8306.

[16] a) C. Ruiz-Perez, J. Sanchiz, M. Hernandez Molina, F. Lloret, M. Julve, *Inorg. Chem.* **2000**, *39*, 1363; b) V. Chandrasekhar, R. Azhakar, B. Murugesa Pandian, R. Boomishankar, A. Steiner, *Dalton Trans.* **2008**, 5962.

[17] a) J. Singh, Ph. D. Dissertation, University of Delhi, **2009**; b) J. Singh, R. Gupta, unpublished results.

[18] *SMART*: Bruker Molecular Analysis Research Tool, Version 5.618, Bruker Analytical X-ray System **2000**.

[19] A. Altomare, G. Cascarano, C. Giacovazza, A. Gualardi, *J. Appl. Crystallogr.* **1993**, *26*, 343.

[20] G. M. Sheldrick, *SHELXL-97*, Program for crystal refinement, University of Göttingen, Göttingen, Germany, **1997**.

[21] G. X. Win, L. J. Fagguria, *J. Appl. Crystallogr.* **1999**, *32*, 837.

Received: March 20, 2009